

## 3D GEOPHYSICAL IMAGING OF THE VAJONT LANDSLIDE AND OF ITS SURROUNDINGS

ROBERTO FRANCESE<sup>(\*)</sup>, MASSIMO GIORGI<sup>(\*)</sup>, GUALTIERO BÖHM<sup>(\*)</sup>, ANDREA BISTACCHI<sup>(\*\*)</sup>,  
ALDINO BONDESAN<sup>(\*\*\*)</sup>, MATTEO MASSIRONI<sup>(\*\*\*)</sup> & RINALDO GENEVOIS<sup>(\*\*\*)</sup>

<sup>(\*)</sup> OGS - Istituto Nazionale di Oceanografia e di Geofisica Sperimentale - Trieste, Italy

<sup>(\*\*)</sup> Università degli Studi di Milano Bicocca - Department of Earth and Environmental Sciences - Milan, Italy

<sup>(\*\*\*)</sup> Università degli Studi di Padova - Dipartimento di Geoscienze - Padua, Italy

Contact author: roberto.francese@inogs.it

### ABSTRACT

The 1963 collapse of the northern slope of the Monte Toc in the Vajont reservoir is probably one of the most studied landslides worldwide. During the various studies several numerical models have been proposed to explain the collapse dynamics but a comprehensive and reliable insight into the failure kinematics is still missing. A major step forward in the understanding of the landslide mechanisms is represented by the reconstruction of the geometry of the different geological units within the landslide body and of the associated physical properties. A large scale geophysical experiment based on 2D and 3D seismic and resistivity was undertaken to address the issue. Prior to the main survey electrical resistivity and longitudinal and transversal wave velocity of the lithological units involved in the landslide were measured along the exposure of the rock wall below the village of Casso. The geophysical images of the two landslide lobes showed a very good correlation with the reference section. Particularly a conductive unit located in the bottom part of the stratigraphic sequence resulted an excellent geophysical marker. Some important structural records, recently defined on the sliding surface, were imaged in the geophysical profiles of the western lobe indicating a limited internal deformation along the east-west axis during the slide. In the deeper part of the western lobe the geophysical image appears rather complicated because of the partial overlap of the various lithological units occurred during the

slide. In the eastern lobe the geophysical images clearly outlined several detachment planes that disrupt the continuity of the pre-landslide geology. The seismic and the resistivity tomography obtained inverting the data resulted comparable indicating a proper choice of the measuring techniques and of the field parameters.

**KEY WORDS:** *Vajont landslide, 3D geophysical imaging, seismic velocity, electrical resistivity, Southern Alps*

### INTRODUCTION

The Vajont area has been studied in details before and after the occurrence of the 1963 catastrophe. It is well known that in the late evening of October 9th the northern slope of the Monte Toc collapsed causing almost 2000 victims mainly in the Piave valley where the huge wave that overtopped the dam wiped out the town of Longarone and several other small villages. The discovery of the palaeo-landslide in 1959 (GIUDICI & SEMENZA, 1960), at the time of the dam construction, was a major impulse in the study of geology, of seismicity and of morphology of the Vajont valley (MÜLLER, 1959; GIUDICI & SEMENZA, 1960; SEMENZA, 1960). Many others data were collected in the following 50 years (ROSSI & SEMENZA, 1965, MARTINIS, 1978; HENDRON & PATTON, 1985; SEMENZA & GHIROTTI, 2000) as the Vajont was one of the most catastrophic landslides occurred in the modern times in the western world. An updated and comprehensive review is given by GENEVOIS & GHIROTTI (2005).

Although several extensive studies were carried out since the 1963 event and many authors proposed different theories to explain the failure and the collapse behaviour (KILBURN & PETLEY, 2003; PETLEY & PETLEY, 2006) some of the factors controlling triggering and dynamic of the landslide are still not completely clear (BISTACCHI *et alii*, in this volume). Among the major issues there is the velocity of the sliding mass itself that caused such an unexpected large wave.

The accuracy of the geological (ROSSI & SEMENZA, 1965) and topographic data (SEMENZA, 2001) collected before the failure allow for a detailed modelling of the geometry and partially also the dynamics of the mass movement. An important improvement of the collapse model and an initial validation of the associated theories could be obtained by a better characterization of the geometry and of the physical properties of the different geological units embedded in the landslide body. For the above reasons a major geophysical exploration program of the Vajont landslide and of its surroundings, based on 2D/3D seismic and resistivity imaging, was undertaken. The geophysical experiment focuses on two points: a) comparing P- and S-wave velocity and resistivity fields of the various lithological units inside and outside the landslide zone; b) mapping the hidden geometry of the various lithological units within the landslide body.

Presently very few geophysical data are available for the Vajont area. Some P-wave profiles were collected before the 1963 collapse, on the palaeo-landslide, to assess the rock quality and few others during the following years to confirm the reliability of the pre-1963 results.

The new geophysical investigation reported here was designed and conducted integrating the re-interpreted geological (BISTACCHI *et alii*, in this volume) and structural data (MASSIRONI *et alii*, in this volume) as well as aerial radiometry and aerial and terrestrial laser scanning data. These last two datasets were extremely useful to constrain the inversion of resistivity and seismic data and model the deformation of the electrical field caused by the rough topography of the landslide mass. The reliability of the new geophysical images is discussed in details and a correlation between lithology and physical parameters is proposed both for the outcropping in-situ bedrock sequence and for the landslide mass. This 3D physical model of the landslide introduces a series of new constrains for an accurate numerical simulation of the landslide kinematics.

## GEOLOGICAL SETTING

The stratigraphy of the Vajont valley is comprised of the typical Jurassic-Cretaceous carbonate sequences of the South-Eastern Alps. The different formational units have been widely described in several papers (CARLONI & MAZZANTI, 1964; SEMENZA, 1965; MARTINIS, 1978) with minor differences in the geological interpretation. The thickness of the formations changes along and across the valley primarily due to a depositional hiatus dated to the Late Jurassic - Early Cretaceous. The Jurassic sequence (Fig. 1) is comprised of the massive Vajont Limestone (350-400 m), of the layered cherty limestone of the Fonzaso Formation (10-40 m) and of the nodular limestone of the Ammonitico Rosso Formation (0-15 m). This latter unit is not continuous and is reported only by some authors. The Cretaceous sequence is comprised of the Soccher Limestone (200-250 m) and of the layered marly limestones and marls of the Scaglia Rossa Formation (ca. 300 m). The units involved in the landslide are the upper part of the Fonzaso Formation and the Soccher Limestone Formation. In these last two Formations ROSSI & SEMENZA (1965) further defined six lithological members indicated with letters from *a* to *f* in Fig. 1.

In the upper part of the Fonzaso Formation (unit *a'*) thin clayey interbeds (from few centimetres to decimetres) are reported in the layered cherty limestone (HENDRON & PATTON, 1985). These interbeds were indicated by HENDRON & PATTON (1985) as the stratigraphic level where the primary sliding occurred caused by overpressured groundwater. There are just few outcrops of this unit as during the collapse the unit was somewhat crunched along the sliding surface. Unit *a''* is comprised of an alternation of layered cherty limestone and marly limestones. According to ROSSI & SEMENZA (1965) the bottom level of unit *a''* is represented by the nodular limestones of the Ammonitico Rosso Formation. Unit *b* is a thin conglomerate layer and is very important because it is a stratigraphic marker both within the landslide and in the surroundings outcrops. Units *c*, *d* and *e* are comprised of massive limestones grading to layered marly and cherty limestones. Finally unit *f* is comprised of layered marly cherty limestones.

The landslide body is comprised of three major lobes (SEMENZA, 1965): the Massalezza lobe and two separate masses (defined as the "eastern lobe" and the "western lobe") failed at a latter time after the wash-out of the Massalezza lobe.

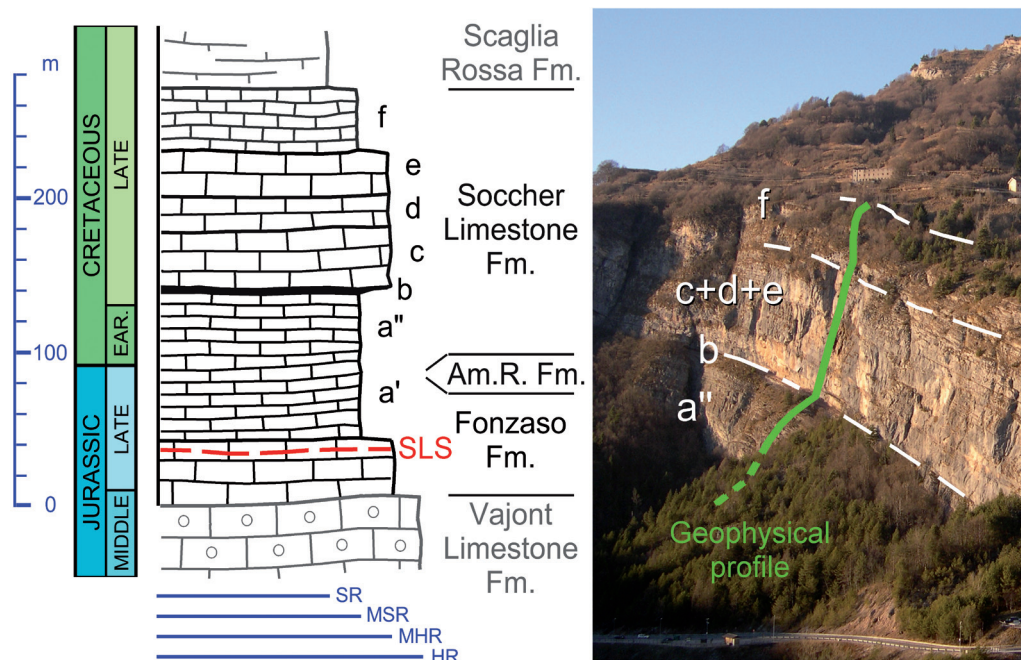


Fig. 1 - Stratigraphy of the Vajont landslide and of its surroundings (left), members indicated with letters from a to f have been originally defined by ROSSY & SEMENZA (1965) and were involved in the landslide. Am.R. = Ammonitico Rosso. SLS = Sliding surface. Unit b (the conglomerate layer) is a stratigraphic marker and it appears as a compact layer located just above the terrace. The horizontal scale represents an attempt of rock quality assessment based on lithology and bedding thickness. SR: Soft Rocks; MSR: Moderately Soft Rocks; MHR: Moderately Hard Rocks; HR: Hard Rocks. Members a" to f as they appear in the rock wall below the village of Casso (right)

Under the structural point of view a review of available data and new observations has been recently completed (MASSIRONI *et alii*, in this volume). In the northern slope of the Monte Toc there is the interference of the well known E-W trending Erto syncline (GIUDICI & SEMENZA, 1960) and of a N-S trending syncline with its axis elongated along the pre-landslide Massalezza valley. The interference is clearly visible in the exposed sliding surface where a series of small and medium scale N-S trending structures fold the Erto syncline. The same folding pattern is also visible outside the landslide area (BISTACCHI *et alii*, in this volume). These structural features appear to have a strong influence on kinematics of the landslide (CASTELLANZA *et alii*, in this volume). In particular the association of the stratigraphy and of the N-trending bedding planes with the curved shape of the sliding surface appeared to be the key factors for the 1963 collapse.

## THE GEOPHYSICAL DATABASE

The effectiveness of the geophysical experiments and of the associated 2D and 3D measure-

ments on the body of the Vajont landslide strongly depends upon the definition of a reliable and accurate physical reference model of the upper part of the Fonzaso Formation and of the Soccher Limestone Formation. This model represents the key to tie the geophysical response (in this case seismic and electrical properties) to lithology and to understand the buried geometry of the different units in the landslide and furthermore to get some insight in the degree of fracturing of the landslide mass itself. The coherency of the rocks could be used as a first indicator of their geo-physical properties. Hard rocks (HR in Fig. 1) are probably characterized both by high velocity and high resistivity while soft rocks (SR in Fig. 1) are low velocity and low resistivity. In this simplified approach units a', a" and f could be classified as moderately soft rocks while units b, c, d and e are mostly referable to moderately hard rocks.

Some boreholes, drilled after the 1963 event (Fig. 3), could be used as a major constrains in assisting geophysical data analysis and processing. The majority of these boreholes reached the depth of

the in-situ bedrock but, unfortunately, the stratigraphy of several wells is not reported in the scientific literature.

The few geophysical data available for the Vajont area refer to P-wave profiles. A seismic survey was conducted immediately after the discovery of the paleo-landslide (CALOI & SPADEA, 1960) in the northern slope of the Monte Toc. Survey results showed surprisingly high (5000-6000 m/s) P-wave velocity values in the uppermost layers indicating potential data inconsistencies (SEMENZA, 1965). A second seismic survey was carried out immediately later than the discovery of the perimetrical crack in October 1960 (SEMENZA, 2001). More realistic P-wave velocity values (2500-3000 m/s) were measured during this second survey. After the 1963 collapse the Court of Belluno required a new seismic survey with the major goal of collecting data inside and outside the landslide area. P-wave velocity was measured at few locations inside (from borehole to borehole) and outside the landslide area (MORELLI & CARABELLI, 1965). The two datasets are not directly comparable because the travelpath in the boreholes crosses different geological units. P-wave velocity values of the Cretaceous sequence outside the landslide range from 2100 m/s to 3000 m/s. These numbers are

quite realistic and more and less similar to the values measured during the second seismic survey.

Seismic velocity and electrical resistivity of a medium depend mostly upon lithology (density), porosity/fracturing and fluid content (TELFORD *et alii*, 1990; DOBRIN & SAVIT, 1988). Fluid content in the Vajont landslide body is almost zero due to the very high permeability of the collapsed mass. This is confirmed by the absolute absence of water in the boreholes. Repetitive attempts to measure the water level during the geophysical campaign were made but a water table has been never detected. The groundwater table in the landslide body is probably controlled by the water level in the residual lake. In the system there are still two unknowns (lithology and porosity/fracturing) and one equation (P-wave velocity or resistivity). To reduce the uncertainty resistivity and P-wave velocity should be measured on the same formations but outside the landslide.

On the rock wall below the village of Casso (Fig. 1) there is a full exposure of units from *a''* to *f* (almost the entire sequence involved in the landslide). A reference geophysical profile was collected here to gain a specific insight in the properties of the different geological units. The only missing unit is *a'* that's covered by the talus deposits.

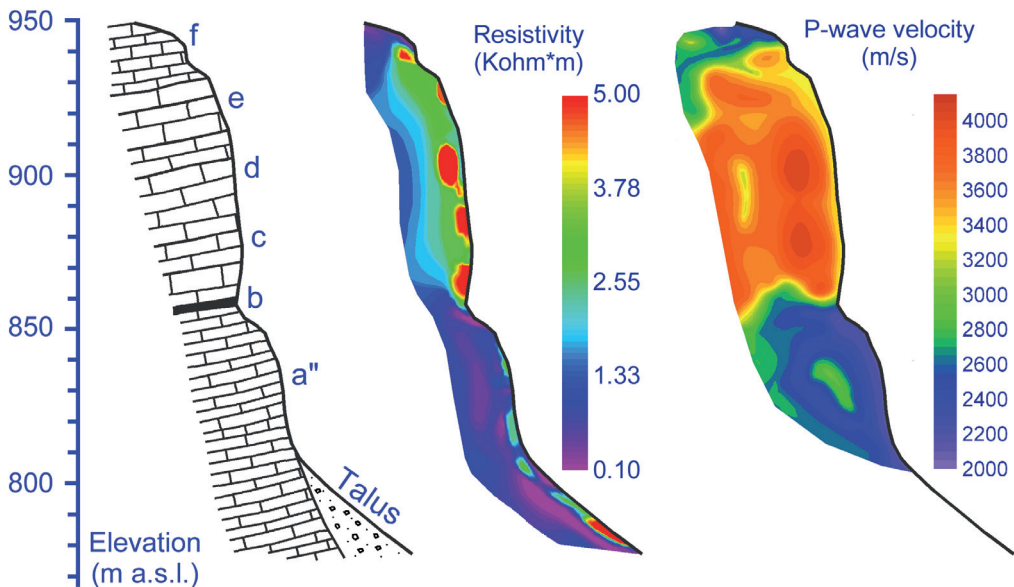


Fig. 2 - Geophysical imaging on the rock wall below the village of Casso. The measuring lines have been deployed on the exposures of Fig. 1. Lithological units *a''* to *f* in the Soccher Limestone Formation (left). Resistivity response (middle) and P-wave seismic response (right)

## GEOPHYSICAL DATA ACQUISITION AND PROCESSING

Geophysical data acquisition was somewhat challenging because of the complex morphology of the landslide and the associated complications in coupling geophones and electrodes especially when the soil was comprised of hard rocks.

The reference profile (Fig. 1 and Fig. 2) was comprised of a 24-channel seismic line and of a 48-electrode resistivity line. In the seismic signal was detected using 10-Hz three component sensors spaced of 10 m while the electrodes, in the resistivity line, were spaced of 5 m and data were recorded using the Wenner and the Dipole-Dipole configurations. Coupling of the seismic sensors and of the electrodes was achieved drilling a series of holes in the rock wall. Geophones were firmly tightened to climbing screws while the electrodes were hammered into holes filled with conductive medical gel. Data resulted good quality and the tomographic inversion of both the two datasets was carried out with a minor misfit (less than 5%). The seismic line resulted a little bit shorter (210 m) as compared to the electrical line because the bottom 4

channels were not connected to the amplifier. The bottom 8 channels of the resistivity line were deployed in the talus deposits (Fig. 2).

Seismic data were collected on the Massalezza lobe only (lobe A in Fig. 3) using a DMT Summit modular system with more than 200 double channel A/D conversion units. Each receiving station was equipped with a three component 10-Hz geophone to detect the incoming signal. The three component sensors were laid out along four lines (L100, L200, L300, L400). The average station spacing was 10.0 m for a total of 276\*3 live channels (Fig. 3). Elastic waves were generated and propagated into the ground using a truck-mounted IVI Minivib vibrating source (both in P-wave and S-wave modes). The sweep was set to 15 s with a frequency ranging from 10 to 350 Hz. The triggering signal was radio transmitted to the command console. The source stations were located along the boundary roads with an average interval of 20 m (Fig. 3). The resulting dataset was comprised of 162 shots covering an area of approximately 500,000 square metres.

Recorded seismic data were generally of good quality; first breaks, in P-wave mode, were sharp and

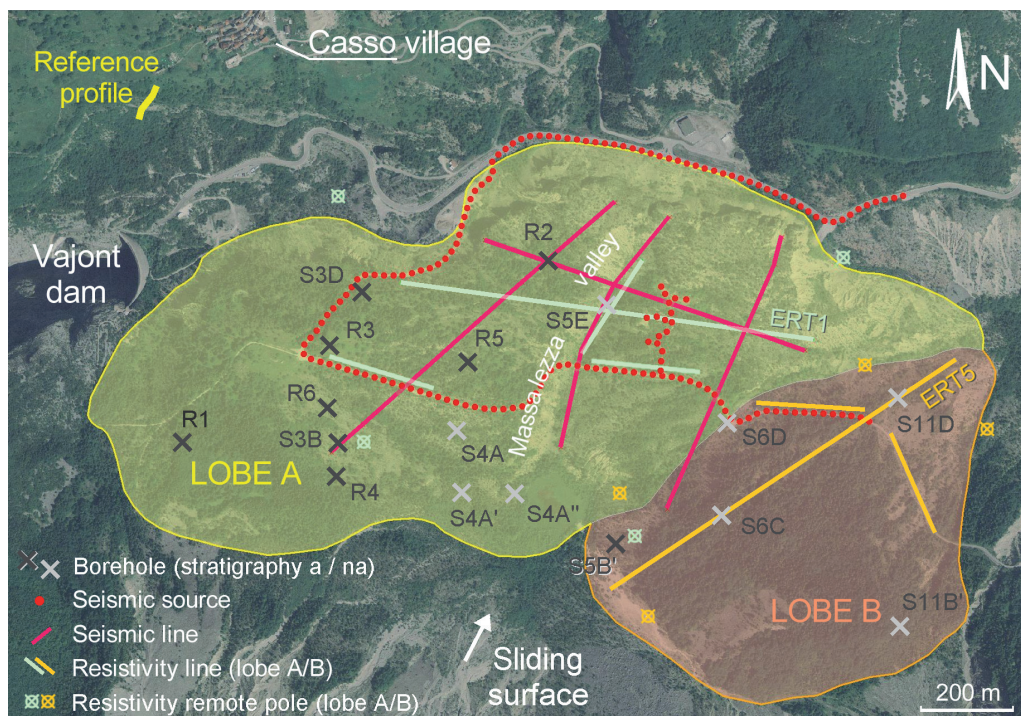


Fig. 3 - Key features of the geophysical campaign on the Vajont landslide (rem. Pole = remote pole; stratigraphy a / na = borehole with "available / not available" stratigraphy)

easy to pick even at offsets larger than 500 m while in S-wave mode the signal was slightly lower amplitude. In P-wave mode a total of about 55000 travel-times were picked and pre-processed prior to invert the data using a combined 3D refraction/reflection tomography. Inversion was carried out with the CAT3D proprietary software. A staggered grid approach (VESNAVER & BOHM, 2000) was utilised to improve the horizontal and vertical resolution in the inverted dataset.

Resistivity data were collected on the two landslide lobes (A and B in Fig. 3) using a 48-electrodes Syscal R1 system. A 2D line, with 20 m electrode separation, was collected approximately in the middle of the lobe and recorded in Wenner configuration. Additional 3D data were collected in Pole-Dipole configuration with four remote poles located in the vicinity of the boundary of the single lobe. Each resistivity volume was comprised of approximately 6000 data-points. Several others 2D lines, with 5 m electrode spacing, covered significant zones within the landslide. In order to minimize the effects of important changes in the water content resistivity data were collected in separate sessions during early spring and middle autumn after three days of heavy rain. The wet soil conditions significantly improved the coupling of the electrodes.

Resistivity data also resulted of good quality and just few points needed to be removed from the dataset prior to run the 2D/3D inversion. Bad data-points removal was mostly focused on the Q values larger than zero and on the high geometric factors (K). Few data points were further removed because of instrumental noise. The inversion was carried out using the package ERTLAB+ that is based on a sophisticated reweight of the inversion parameters after each iteration (MORELLI & LABRECQUE, 1996).

## RESULTS AND DISCUSSION

### THE REFERENCE PROFILE

Unit *a''* in the lower part of the rock wall appears to be low-velocity (2200-2700 m/s) and low-resistivity (0.5-1.1 Kohm\*m). The raising of the near surface resistivity in the elevation interval 780-800 m is due to the coarse pebbly deposits of the talus debris. Unit *b*, due to its reduced thickness (less than 4 m), is outside the resolution capability of both the two techniques. Units *c*, *d* and *e* in the middle part of the rock wall appear to have a similar response. In these units the velocity (3400-3800 m/s) and the resistivity (2.5-4.5

Kohm\*m) are higher as compared to unit *a''* indicating the massive character of the limestones. At least three very resistive domains are visible in the resistivity image. The consistency of the rocks in these zones is probably very high and much higher with respect to the average of the middle portion of the rock wall. At the top of the rock wall, where unit *f* outcrops, there is a sudden lowering of both the resistivity (0.5-1.0 Kohm\*m) and the velocity (2300-2800 m/s).

### THE LANDSLIDE BODY

In the inverted 2D and 3D dataset the vertical and horizontal resolution could be approximately 10 m in the vicinity of the geophysical lines. The depth of investigation of both the seismic and the resistivity data, although sufficient to detect the in-situ bedrock, was not adequate to resolve it.

Resistivity in the landslide body ranges from 0.15-0.20 Kohm\*m to values larger than 3.50-4.00 Kohm\*m.

The resistivity image along the 2D profile ERT1 (Fig. 4) appears to be quite complicated. The tri-dimensional geometry of the geological structures associated with the nature of the electrical field that has a similar sensitivity below and on both the two sides of the profile generated a complex response. Resistivity values (ranging from 0.25 to about 3.0 Kohm) appear to be slightly lower as compared to the reference profile. This is probably related to the high degree of fracturing of several units within the landslide. Unfortunately along profile ERT1 there are no borehole data available to constrain the interpretation. Stratigraphy of borehole S5E was not found in the literature

In order to achieve a reliable interpretation the deep conductive unit *a''* (Fig. 4) was utilized to define the geological layout along the profile. The most prominent structure is a narrow syncline fold located in the middle portion of the profile with its axis probably elongated along the old Massalezza valley. The structure is consistent with the one of the in-situ bedrock visible in the scarp area. The bottom layers are probably belonging to the *a''* unit while in the top layers there are the typical lithologies of the *c* unit; the high resistive uppermost layer is a thick fluvio-glacial deposit exposed at different spots in the Massalezza valley. In the left portion of the profile are visible some resistive bodies that could be associated with a partly undifferentiated c-d-e lithological sequence. The near

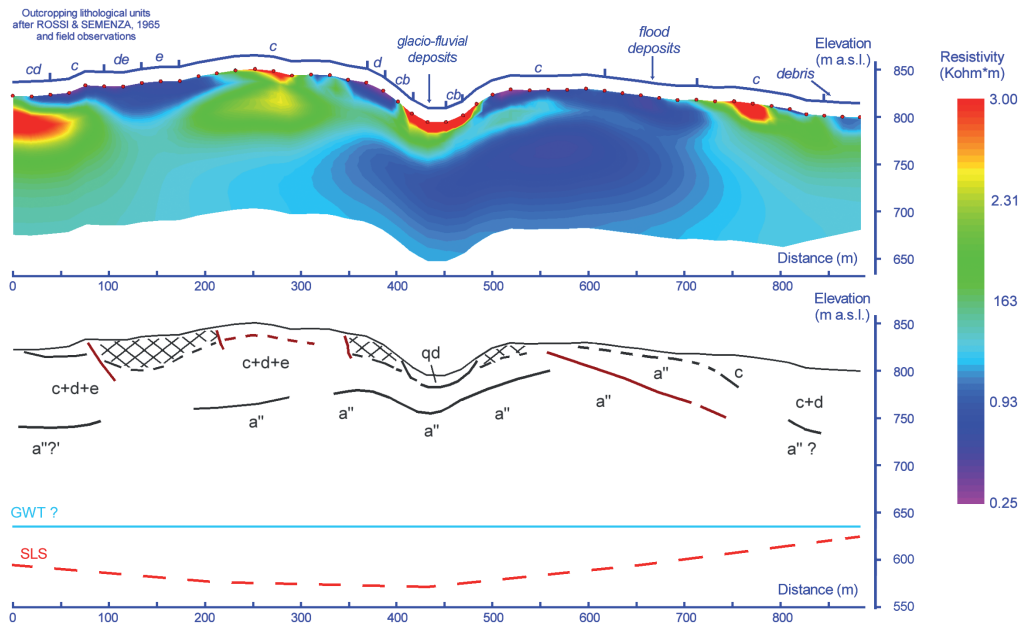


Fig. 4 - 2D Resistivity image along tomography ERT1 (top). Profile is oriented from W to E (see Fig. 3). Preliminary interpretation (bottom). Letters from a to f represent the lithological units as defined by ROSSI & SEMENZA (1965); Electrical resistivity in unit a'', ranges from 0.50 Kohm\*m to 1.10 Kohm\*m while in the c-d-e sequence it ranges from 1.7 Kohm\*m to values larger than 2.0 Kohm\*m. The lowering of the resistivity in the c-d-e sequence (as compared to the reference section) is probably due to severe fracturing. qd: quaternary deposits. SLS: sliding surface. The groundwater table (GWT) probably corresponds to the water level in the residual lake (635 m a.s.l.) The investigated landslide mass could be then considered dry. See text for description

surface conductive unit, visible in the interval 50-200 m, according to ROSSI & SEMENZA (1965) still belongs to units c, d and e. In this case either the mass is very fractured or unit d in the landslide is more conductive than in the reference section. In the eastern section of the profile, starting from the x-coordinate 550 m, there is a clear overlapping of a near surface conductive body on the eastern flank of the deep a'' unit.

In profile ERT1 the resistivity contacts are folded with an apparent N-S trend (Fig. 4). According to MASSIRONI *et alii* (in this volume) these structures, clearly visible in the sliding surface, were surprisingly preserved in the landslide body confirming the hypothesis of a sliding mode with marginal disturbance of structural features. Furthermore the c-d-e sequence exhibits a larger thickness as compared to the reference section. This is probably due to a duplication of the units caused by some detachment phenomena occurred, during the failure, along existing or newly developed discontinuities. Some of these high angle discontinuities have already been reported by ROSSI & SEMENZA (1965) but there are also some others low

angle detachment planes (see for example at the x-coordinate interval 200-300 m) that could explain the larger thickness of the c, d and e units in depth.

The resistivity image along profile ERT5 (Fig. 5), that intersects lobe B, shows a framework more and less comparable with the post-failure geological map of ROSSI & SEMENZA (1965). The outcropping lithological layers are represented by an undifferentiated unit a covering almost the entire Col Tramontin (located approximately in the centre of lobe B of Fig. 3) and by some smaller spots belonging to the unit b. The general structure appears to be folded with some major internal discontinuities. In this case also the stratigraphy of boreholes S6C and S11D was not available to constrain interpretation. The geometry of the bottom layers of lithological unit a'' was utilized as a geophysical marker to define the geological layout. In the reference section (Fig. 1) unit a' is not exposed and hence there are no indications about its possible geophysical response. Regarding the thickness of lithological units a' and a'' former indications from CARLONI & MAZZANTI (1964) suggest a total

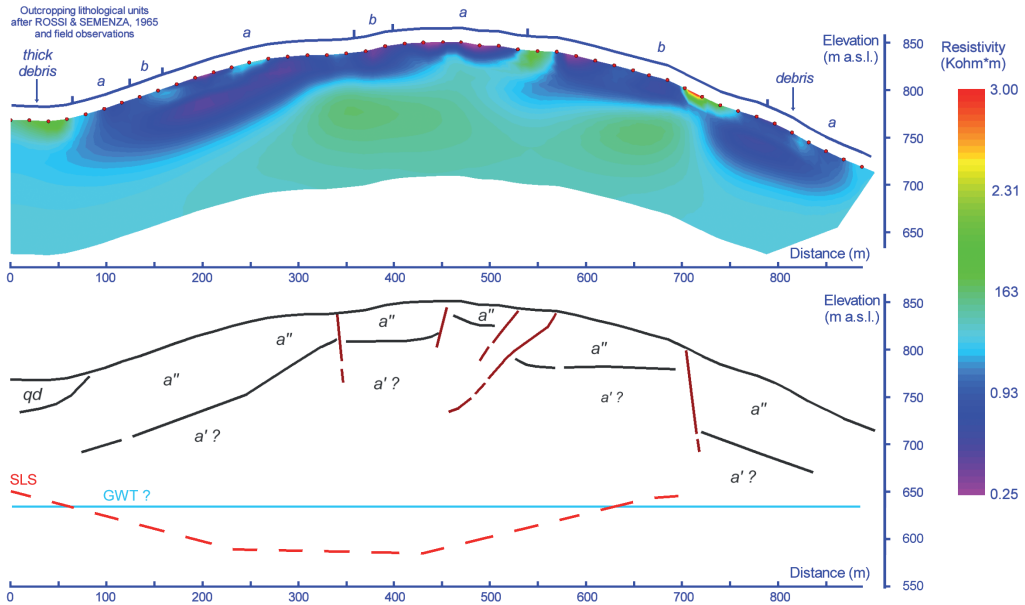


Fig. 5 - 2D resistivity image along tomography ERT5 (top). Profile is oriented from SW to NE (see Fig. 3). Preliminary interpretation (bottom). Letters from a to f represent the lithological units as defined by ROSSI & SEMENZA (1965); Electrical resistivity in unit a", ranges from 0.50 Kohm\*m to 1.10 Kohm\*m. qd: quaternary deposits. Reference resistivity values for unit a' are not available. SLS: sliding surface. The groundwater table (GWT) probably corresponds to the water level in the residual lake (635 m a.s.l.) The investigated landslide mass could be then considered dry. See text for description

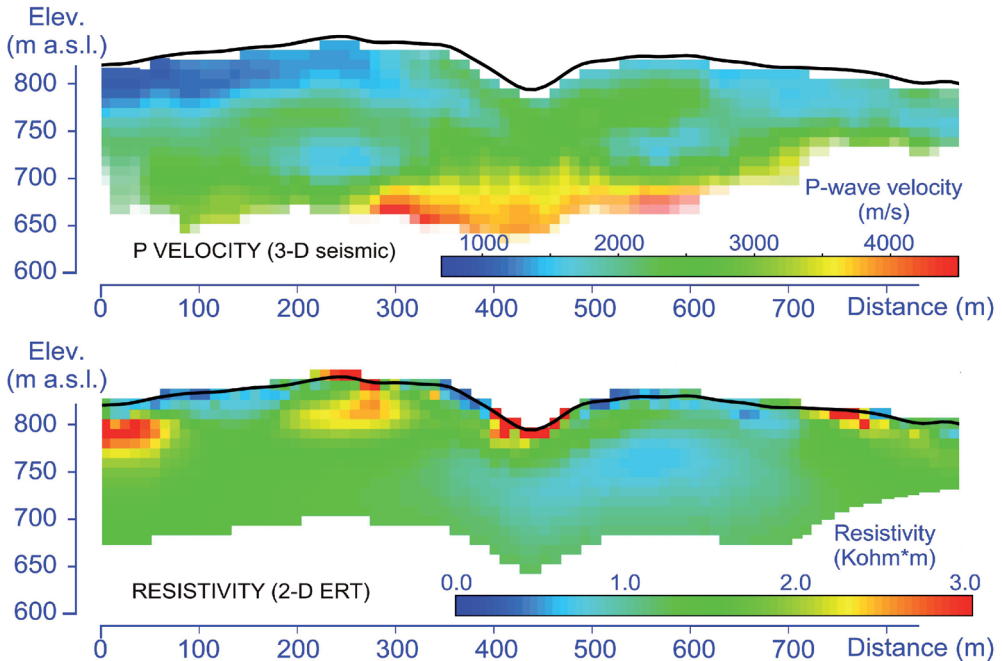


Fig. 6 - Comparison between 3D seismic (tomography (top) and 2D electrical tomography (bottom) response. The profiles are oriented from W to E. The geophysical data are presented as 10m by 10m cell scalars without interpolation. The two sections are computed along the trace of profile ERT1. See text for description



thickness of about 80-90 for the undifferentiated unit  $a$ . The maximum thickness of unit  $a''$  is around 50 m. According to several authors (ROSSI & SEMENZA, 1965; MARTINIS, 1978; HENDRON & PATTON, 1985) unit  $a'$  is similar to unit  $a''$  with the sole difference of the presence of some thin interbedded clays in the basal layers. The resistivity signature of units  $a'$  and  $a''$  should be then comparable. Regarding these considerations the increase of the resistivity values in the deeper portion of profile ERT5 appears rather difficult to explain. There are basically two ways to interpret this behaviour. In the first case the upper part of unit  $a'$  is more resistive than expected (Fig. 5) while in the second and more realistic case in the deeper portion of profile ERT5 unit  $a''$  overthrusts the resistive terrains belonging to the  $c-d$  units. As mentioned above several high and low angle discontinuities are clearly visible in the profile. These planes disrupt the former continuity of the geological layers generating an ensemble of pop-up like structures. Unfortunately on this lobe the sliding surface is not constrained by post-landslide data and also during the failure occurred a partial overlap of the eastern lobe on the western one. The deeper portion of the geophysical image could be then really complex.

The P-wave velocity values in the landslide body range from 700-1000 m/s to values larger than 3500-4000 m/s in those spots where the rocks are still very compact. Seismic data resulted comparable to electrical data with a reasonable degree of confidence.

The correspondence between resistivity and P-wave velocity has been analysed in details along profile ERT1 (Fig. 6) on lobe A of the landslide. The P-wave profile was extracted from the 3D subsurface velocity model while the resistivity data belongs to a standard 2D acquisition. A 3D resistivity volume of lobe has been also generated with the aid of four remote poles (Fig. 3) and although the data quality is encouraging it has not been yet analysed in details.

The syncline structure below the Massalezza ditch is visible also in the seismic data but it is not completely resolved as in the resistivity image probably because the geophone line is located 60 m northern of the electrode line. Right in the middle of the P-wave section there is a high-velocity bottom layer that is not visible in the resistivity section. The high-velocity layer is located at a depth where the signal to noise ratio of the resistivity data is very low. It is known that a

deep resistive layer below a conductive layer requires very large AB spacing to be sampled by an electrical field that is forced into the conductor. The seismic data are reliable because there is a geophone line exactly along the Massalezza ditch (Fig. 3) and the sources are located on the nearby road. According to the previous consideration a high velocity layer (or high resistivity) below unit  $a''$  is quite difficult to explain without assuming the presence of a detachment plane that duplicate the sequence. In the right side of the velocity profile there is an east-verging structure that is also visible in the resistivity section. The near surface high-resistivity values that have no correspondence in the seismic image are due to the presence of debris with a large percentage of voids. In the left side of the velocity profile there are some observable differences between P-wave velocities and resistivity values. The near surface is low velocity in the uppermost 30 m and this low velocity layer is laterally continuous while in the electrical section two high-resistivity zones are visible. The difference is probably due to the averaging effect of the algorithm (diving wave) used to invert the seismic volume. The stratigraphy of the key boreholes is not presently available to constrain the geophysical interpretation. A possible strategy to minimize this limitation was to compare the different geophysical responses and also to compare the geophysical data with the surface geology.

## CONCLUSIONS

The 2D and 3D geophysical parameterization of large landslide accumulation masses represents a great challenge because the displacement of the geological/lithological units generally occurring during the failure and often corresponding to a high complexity in the spatial distribution of the physical properties within the landslide body. The Vajont landslide makes no difference and because of its size is also more complicated. The geophysical investigation was undertaken with a large effort and it is still in progress but the authors are aware that in various areas of the landslide the resolution should be increased. This last issue is vital to support a reliable subsurface reconstruction and hence proper modelling of the landslide dynamics. Although geology has been studied in details before and after the failure the geometry of the buried units it is still partially unknown. Borehole stratigraphy is only partially reliable because there are no evident markers and also

correlating well information in such a laterally variable environment is very critical. The microfossil logs in the boreholes confirm the existence of several detachment planes that cause sequence duplications.

The different units involved in the landslide, due to the lithological changes were expected to have a distinct geophysical signature. The seismic and resistivity profiles collected along the rock wall below Casso confirmed this hypothesis and the landslide sequence from the bottom to the top is a sort of sandwich of conductive (low velocity) - resistive (high velocity) - conductive (low velocity) layers. No reference data were collected for the 35-40 m thick bottom unit *a'* as it was not exposed along the reference section.

Resistivity and seismic imaging within the landslide body confirmed the general observations from the reference section. The conductive unit *a''*, because of its position in the sequence that is just below the stratigraphic marker *b*, was chosen as a geophysical marker for the initial interpretation. The pre-landslide stratigraphy appears well preserved in the very near surface layers, but in depth the geophysical response often exhibits complex images. In the subsurface of lobe A both the resistivity and the seismic images along profile ERT1 traced a syncline structure that was also recognized in the exposed record of the sliding surface. In addition in the same profile the geophysical layout shows a series of other small-scale folds compatible with a stress field acting along the east-west direction. These structures are probably pre-landslide as the stress occurred during

the 1963 failure and before at the time of the former landslide was acting in the north-south direction. This is clearly visible in resistivity profile ERT5, collected on lobe B, where the entire geophysical layout appears to be affected by folds with east-west axes.

The quaternary coverage, mostly glacial and talus deposits with a thickness of few to several metres, which could be a major obstacle to reconstruct subsurface geology, did not create any problem for the geophysical investigation. These deposits are generally in dry conditions or just wet after a rainfall. The presence of an abundant silty matrix allowed for a better coupling of the sensors resulting in a minor distortion of the field to be measured.

Further work that will be undertaken in a very near future includes (1) geophysical parameterization of unit *a'*, (2) inversion of the electrical data into a 3D resistivity volume of the entire landslide, (3) correlation of the seismic and of the resistivity responses to improve interpretation and finally (4) processing of S-wave data in order to estimate the elastic parameters of the landslide body.

## ACKNOWLEDGMENTS

We acknowledge the Friuli Venezia-Giulia Region for providing the funding for the project (project 35935/2010). A special thank to Alessia Rosolen for her personal support and to Ketty Segatti. A final thank to Giovanni Rigatto for his assistance during field operations.

## REFERENCES

- BISTACCHI, A., MASSIRONI, M., SUPERCHI, L., ZORZI, L., FRANCESE, R., GIORGI, M., GENEVOIS, R. & CHISTOLINI, F. (2013) - *A 3D Geological Model of the 1963 Vajont Landslide*. In this volume.
- CALOI, P. & SPADEA, M., C. (1960) - *Serie di esperienze geosismiche seguite in sponda sinistra a monte della diga del Vajont (dicembre 1959)*. SADE Technical Report.
- CARLONI, G., C. & MAZZANTI, R. (1964) - *Rilevamento geologico della frana del Vajont*. In: SELLI R. et alii. *La frana del Vajont*, *Giornale di Geologia*, 2: 32/1.
- CASTELLANZA R., AGLIARDI F., BISTACCHI A., MASSIRONI M., CROSTA G.B. & GENEVOIS R. (2013) - *3D finite-element modelling of the Vajont landslide initiation stage*. In this volume.
- DOBRIN M.B. & SAVIT C.H. (1988) - *Introduction to geophysical prospecting*. 4<sup>th</sup> edition, McGraw-Hill, 867 pp.
- GENEVOIS R. & GHIROTTI M. (2005) - *The 1963 Vajont landslide*. *Giornale di Geologia Applicata*, 1: 41-52.
- GIUDICI F. & SEMENZA E. (1960) - *Studio geologico del serbatoio del Vajont*. SADE Technical Report.
- HENDRON A.J. & PATTON F.D. (1985) - *The Vajont slide, a geotechnical analysis based on new geological observations of the failure surface*. Tech. Rep. GL-85-5, Department of the Army, US Army Corps of Engineers, Washington D.C., 2 vols.
- KILBURN C.J. & PETLEY D.N. (2003) - *Forecasting giant, catastrophic slope collapse: lessons from Vajont, Northern Italy*. *Geomorphology*, 54 (1-2): 21-32.
- MARTINIS B. (1978) - *Contributo alla stratigrafia dei dintorni di Erto-Casso (Pordenone) ed alla conoscenza delle caratteristiche*

- strutturali e meccaniche della frana del Vajont*. Memorie di Scienze Geologiche, Università di Padova, **32**: 1-33.
- MASSIRONI, M., SUPERCHI L., ZAMPIERI D., BISTACCHI A., RAVAGNAN R., BERGAMO A., GHIROTTI M. & GENEVOIS R. (2013) - *Geological Structures of the Vajont landslide*. In this volume.
- MORELLI C. & CARABELLI E. (1965) - *Misure di velocità delle onde elastiche longitudinali nella roccia del bacino del Vajont*. Court of Belluno. Lerici Foundation. Research 410.
- MORELLI G. & LABRECQUE D.J. (1996) - *Robust scheme for ERT inverse modelling*. European Journal of Environmental and Engineering Geophysics, **2**: 1-14.
- MÜLLER L. (1959) - *Talsperre Vaiont - 6 Geotechnischer Bericht*. SADE Technical Report.
- MÜLLER L. (1964) - *The rock slide in the Vaiont valley*. Felsmechanik und Ingenieur-geologie, **2**: 148-212.
- PETLEY D.N. & PETLEY D.J. (2006) - *On the initiation of large rockslides: perspectives from a new analysis of the Vaiont movement record*. In: SCARASCIA MUGNOZZA G., STROM A. & HERMANN R.L. (Eds.). *Massive Rock Slope Failure*. NATO Science Series, Earth and Environmental Sciences, **49**: 77-84.
- ROSSI D. & SEMENZA E. (1965) - *Carte Geologiche del versante settentrionale del M. Toc e zone limitrofe prima e dopo il fenomeno di scivolamento del 9 Ottobre 1963. Scala 1:5000*. Ist. Geol. Univ. Ferrara, Italy.
- SEMENZA E. (1960) - *Nuovi studi tettonici nella valle del Vajont e zone limitrofe*. Acc. Naz. Lincei, Rend. Cl. Sc. MMFFNN, **8**: 28/2.
- SEMENZA, E. (1965) - *Sintesi degli studi geologici sulla frana del Vaiont dal 1959 al 1964*. Memorie del Museo Tridentino di Scienze Naturali, **16**: 1-52.
- SEMENZA E. (2001) - *La storia del Vaiont raccontata dal geologo che ha scoperto la frana*. Tecomproject Ed., Ferrara, Italy. 279 pp.
- SEMENZA E. & GHIROTTI M. (2000) - *History of the 1963 Vaiont Slide. The importance of the geological factors to recognise the ancient landslide*. Bulletin of Engineering Geology and the Environment, **59**: 87-97.
- TELFORD W.M., GELDART L.P. & SHERIFF R.E. (1990) - *Applied Geophysics*. 2<sup>nd</sup> edition. Cambridge University Press, 770 pp.
- VESNAVER A. & BOHM G. (2000) - *Staggered or adapted grids for seismic tomography?* The Leading Edge, **19** (9): 944-950.

